



Relationship between the ionization and oxidation potentials of molecular organic semiconductors

Brian W. D'Andrade^a, Shubhashish Datta^a, Stephen R. Forrest^{a,*},
Peter Djurovich^b, Eugene Polikarpov^b, Mark E. Thompson^b

^a Department of Electrical Engineering, EQUAD B301, Princeton University, Princeton, NJ 08544, United States

^b Department of Chemistry, University of Southern California, Los Angeles, CA 90089, United States

Received 28 July 2004; received in revised form 11 January 2005; accepted 22 January 2005

Available online 17 March 2005

Abstract

A relationship between the energy of the highest occupied molecular orbital (HOMO) and the oxidation potential of molecular organic semiconductors is presented. Approximating molecules as dipoles consisting of a positively charged ion core surrounded by an electron cloud, the HOMO energy (E_{HOMO}) is calculated as that required to separate these opposite charges in a neutral organic thin film. Furthermore, an analysis of image charge forces on spherical molecules positioned near a conductive plane formed by the electrode in an electrochemical cell is shown to explain the observed linear relationship between E_{HOMO} and the oxidation potential. The E_{HOMO} 's of a number of organic semiconductors commonly employed in thin film electronic devices were determined by ultraviolet photoemission spectroscopy, and compared to the relative oxidation potential (V_{CV}) measured using pulsed cyclic voltammetry, leading to the relationship $E_{\text{HOMO}} = -(1.4 \pm 0.1) \times (qV_{\text{CV}}) - (4.6 \pm 0.08) \text{ eV}$, consistent with theoretical predictions.

© 2005 Elsevier B.V. All rights reserved.

PACS: 73.20.-r; 82.45.Wx; 71.20.Rv; 78.40.Me

Keywords: Electrochemistry; Photoelectron spectroscopy; Organic thin film; Dipole

1. Introduction

Knowledge of charge carrier energy levels in organic thin films is essential for the understanding

and design of organic devices [1]. For example, an organic light emitting device (OLED) usually consists of several layers of various stacked organic thin films [2], and offsets in the energies between layers act as potential energy barriers to the flow of charge and molecular excited states (or excitons). The highest occupied molecular orbital (HOMO) and lowest unoccupied molecular orbital

* Corresponding author. Tel.: +1 609 258 4532; fax: +1 609 258 7272.

E-mail address: forrest@princeton.edu (S.R. Forrest).

(LUMO) energy are used to describe isolated molecules. Energy levels in solid-state organic films, bonded by weak intermolecular interactions, can be derived from these orbital energies. For convenience, we will refer to the derived energy levels in the solid-state as the HOMO and LUMO.

Two conventional methods to ascertain HOMO energies (E_{HOMO}) are ultraviolet photoemission spectroscopy (UPS) [3] and cyclic voltammetry (CV) [4,5]. UPS experiments determine the ionization energy (E_i) of a molecule on the surface of a thin film, where $E_i = -E_{\text{HOMO}}$ [6]. Solution-based CV experiments determine the relative molecular oxidation potentials (V_{CV}), which are indirectly related to E_i . It is therefore desirable to determine E_{HOMO} from UPS data; however, the high cost and complexity of UPS systems tends to favor the use of CV in many laboratories.

In this paper, we explore the relationship between E_{HOMO} determined from UPS of organic thin films, and V_{CV} as determined from cyclic voltammetry. Previous studies [7–9] consider solid and solution state solvation effects to approximately describe this relationship. In this work, the relationship is explained using a simple electrostatic model that takes into account the additional effect of image charges, thereby allowing for an accurate and *quantitative* comparison between these independently measured quantities for a broad range of molecules of interest in organic electronics.

A description of the individual techniques along with their relative strengths and weaknesses is given in Section 2. A quantitative theory of the relationship between E_{HOMO} and V_{CV} as measured by UPS and CV, respectively, is developed in Section 3, and experimental procedures are given in Section 4. Results and discussion of the analysis are in Section 5, and conclusions are provided in Section 6.

2. Ultraviolet photoemission spectroscopy and cyclic voltammetry

In UPS, ultraviolet light is incident on a thin film sample, ejecting electrons from its surface. The kinetic energy of the electron varies according

to its molecular orbital, and the sum of the absolute value of the electron kinetic energy and its orbital potential energy is equal to the photon energy. An electron from the HOMO has the highest kinetic energy [10,11].

A typical organic thin film UPS spectrum of the metallic–organic phosphor *fac*-tris(2-phenylpyridine)iridium [Ir(ppy)₃] due to illumination from the 21.22 eV He I α line is shown in Fig. 1. The HOMO position relative to the vacuum level is estimated by linearly extrapolating the low binding energy side of the spectrum to the zero intensity baseline, corresponding to the intersection of the pair of lines shown. Similarly, the intersection of the lines at high binding energy provides an estimate of the lowest energy electrons. The difference between the two energies is the maximum of the kinetic energy, E_{kin} , of the emitted HOMO electrons at the sample surface, whereby E_{HOMO} is calculated from $E_{\text{kin}} - 21.22$ eV.

In CV, the organic material is dissolved in a solvent containing an electrolyte, a reference solute, and the working, counter and reference electrodes. Voltage is swept across the electrodes, inducing a current. To avoid resistive drops and internal polarization, the voltage measured is that of the

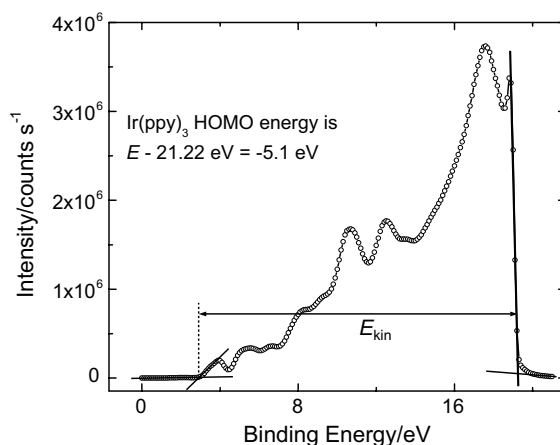


Fig. 1. UPS spectrum of an Ir(ppy)₃ thin film grown on Ag and biased at -3 V. The ionization energy is determined by linearly extrapolating the high and low energy slopes of the spectrum to the spectral baseline, using the four lines shown. The energy separation, E_{kin} , between these two points is subtracted from the photon energy of 21.22 eV to determine the HOMO energy.

working electrode relative to the reference electrode. The sample is oxidized to the +1 state (corresponding to a singly ionized molecule) upon contact with the working electrode, at the voltage corresponding to the average of the anodic and cathodic peak currents. This voltage is related to the energy of the HOMO [5], since only the electron from this orbital is involved in the oxidation process.

An example of a cyclic voltammogram of $\text{Ir}(\text{ppy})_3$ is given in Fig. 2. The reversible oxidation peaks of the reference and sample have positive potential values, and V_{CV} is the difference between the potentials at which the reference solute and samples are oxidized. Also shown are the negative potentials at which the sample is reversibly reduced to its -1 and -2 states.

In cyclic voltammetry, consideration must be given to the effects of the solvent, the electrolyte, the electrodes, and the reversibility of the redox reaction of the sample. The acquisition of an accurate value of V_{CV} requires that the solvent resist oxidation. Furthermore, the electrolyte and electrodes also must not react with the sample, and oxidation of the samples must be reversible, result-

ing in closed current–voltage loops. The potential measured for a reversible redox reaction in a cyclic voltammetry experiment is however a good estimate for the thermodynamic standard oxidation potential with an error on the order of millivolts [12]. In UPS measurements, materials must have a low room temperature vapor pressure to be compatible with the ultrahigh vacuum (UHV) ($\sim 10^{-9}$ Torr) environment, and the films must be chemically and morphologically stable under ultraviolet radiation. Also, inaccuracies in measuring E_{HOMO} can occur from charging of the film and the surrounding UHV apparatus.

The UPS system used in our experiments has a resolution of 150 meV, whereas redox potentials in CV are determined to within 50 meV. UPS measurements made using synchrotron radiation sources can have higher resolutions (~ 20 meV), but their cost is often prohibitive for routine measurements. For CV, the resolution is determined by the error in the voltmeter, the stability of the power source, and the sweep rate; the oxidation reaction must occur on a time scale that is short compared to the voltage cycle time. Neither method probes the bulk ionization energy introducing additional potential measurement uncertainties. As noted previously, UPS only explores the energetics of surface and near-surface electronic states, and CV measures the potential energy of electron orbitals of molecules suspended in an electrolytic environment.

3. Analytical comparison between UPS and CV measurements

We now consider image charge effects between a dipolar molecule suspended in an electrolyte near a conducting, metallic electrode that results in a simple, quantitative relationship between UPS and CV measurements. This effect ignores the details of other solvation effects, the metal workfunction [13,14], details of the molecular frontier orbitals, and the explicit role of the electrolyte [15,16], that have been previously identified as playing a role in the energies from these two techniques. These other factors that contribute to the relationship between the two measurements are simply grouped

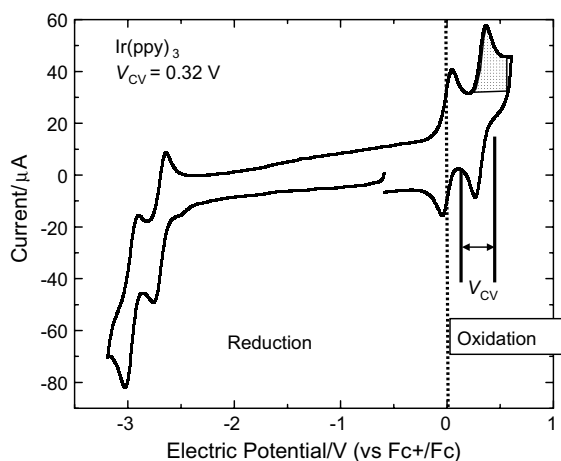


Fig. 2. Example of a pulsed cyclic voltammogram for $\text{Ir}(\text{ppy})_3$. Voltages for the sample and reference solute are recorded as the center voltage between the peak for the oxidation of the sample and the peak for the reduction of the oxidized sample, as shown. V_{CV} is determined from the difference between the oxidation potentials shown.

together and expressed in the form of a ratio of effective dielectric constants. Hence, while the electrostatic model provides an excellent fit to the observed trends, it does not strive to explain the detailed effects nor the physical origins of these other contributions, but rather assumes that their contribution is accounted for in the details of the macroscopic dielectric constant of the electrolytic solution.

Molecular oxidation is studied in UPS by considering the energy required to singly ionize a molecule on the surface of a film of relative dielectric constant, ϵ_{film} . We approximate a molecule as a positive ion core surrounded by an electron cloud with an effective radius, r . The oxidative potential measured by UPS is therefore given by the Coulomb energy:

$$U_{\text{UPS}} = E_{\text{HOMO}} = -\frac{1}{4\pi\epsilon_0\epsilon_{\text{film}}} \cdot \frac{q^2}{r}. \quad (1)$$

Here, q is the electron charge, and ϵ_0 is the permittivity of vacuum.

Image charge effects have been shown to reduce the HOMO energy levels relative to the vacuum level for thin monolayers in UPS experiments [6], and they can be used to explain the relationship between the work function and ionization energy of metals [17]. In CV measurements, molecules are in contact with a conductive electrode, so the dipole arising from image charges of the molecular ion core and the electrons should also play a significant role. Additionally, the molecules are dissolved in a dielectric solution; hence, the solvation effect is also an important consideration [18,19]. With the inclusion of the conducting, planar electrode, the equipotential surface around the positive molecular core can be approximated as a sphere whose center is displaced from the electrode due to the image, thereby reducing the total potential energy. To estimate E_i as measured by CV, we approximate the molecule as having an electron occupying an equipotential sphere of effective radius, r , with a positive core at a distance, d , from the conducting electrode, as shown in the inset, Fig. 3. The molecular dipole induces its image in the electrode. This results in an apparent offset of the core charge ($+q$) by a distance, Δ , as shown. Equating the potential of a conducting surface at

the points nearest and farthest from the electrode, the molecular potential as measured by its oxidative voltage is

$$\begin{aligned} V_{\text{OX}} &= V_{\text{CV}} + V_{\text{REF}} \\ &= \frac{q}{4\pi\epsilon_0\epsilon_{\text{CV}}} \left[\frac{1}{r - \Delta} - \frac{1}{2d - r + \Delta} \right] \\ &= \frac{q}{4\pi\epsilon_0\epsilon_{\text{CV}}} \left[\frac{1}{r + \Delta} - \frac{1}{2d + r + \Delta} \right], \end{aligned} \quad (2)$$

where V_{REF} is the oxidation potential of the reference solute used in cyclic voltammetry, and ϵ_{CV} is the effective dielectric constant near the electrode, which is a function of both the dielectric constant of the solvent, ϵ_{Sol} , and the screening from the electrolyte. The shift between the core and the center of the electron cloud is then given by the positive real root of the following cubic equation:

$$\Delta^3 + (4d + r)\Delta^2 + (4d^2 - r^2)\Delta - r^3 = 0. \quad (3)$$

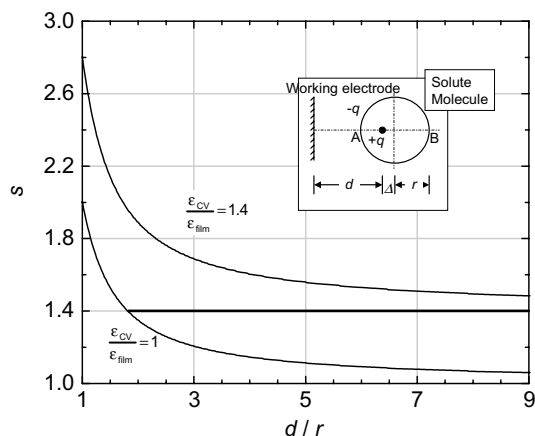


Fig. 3. The rate of change in the HOMO energy of a molecule relative to its oxidation energy ($s = (1/q)|dE_{\text{UPS}}/dV_{\text{CV}}|$), versus the distance from the conductor normalized to the radius of the molecule, d/r , for two extreme cases where either the image charge effect or the solvation effect is solely responsible for the difference in energy levels measured using UPS and CV. The bold line corresponds to possible situations involving both the effects that are consistent with the experimental fit in Fig. 4. *Inset*: Schematic diagram showing an equipotential “molecular sphere” of radius, r , having a charge $-q$, and a $+q$ point charge inside it. Here, Δ is the distance between the center of the sphere and the positive charge which is offset due to induced image charges in the metal electrode.

Comparing Eqs. (1) and (2),

$$V_{CV} = -\frac{E_{HOMO}}{qs} - V_{REF},$$

where

$$s = \frac{\epsilon_{CV}}{\epsilon_{film}} f(r, d)$$

and

$$f(r, d) = \frac{1}{r} \left[\frac{1}{r + \Delta} - \frac{1}{2d + r + \Delta} \right]^{-1}.$$

Generally, ϵ_{CV} is greater than ϵ_{film} due to solvation effects. The slope, s , of a plot of E_{HOMO} versus V_{CV} is then the product of the ratio of permittivities and the image charge factor, $f(r, d)$. The y -intercept of the plot is determined by the reference solute used in the CV measurement. A plot of s as a function of d/r is given in Fig. 3 for two values of the ratio of permittivities. Hence, Eq. (4) provides a quantitative relationship between V_{CV} measured by cyclic voltammetry, and the ionization energy of the molecules under study.

4. Experimental

Silicon substrates used for UPS measurements were oxidized for 5 min in 4:1 $H_2SO_4:H_2O_2$, etched for 2 min in dilute HF, and blown dry with pure nitrogen. The substrates were fastened to copper substrate holders with copper clips, then loaded into the ultrahigh vacuum system.

A 50 nm thick Ag film was deposited onto the substrate and substrate holder, with electrical connection between these surfaces made via the copper clips. Furthermore, the Ag film was used to establish the Fermi energy in the organic film, assuming they are aligned in equilibrium. After Ag deposition, the substrate is transferred under UHV to the organic deposition system [20].

Prior to film growth, organic materials, purified by train sublimation [21], were outgassed and loaded into the growth chamber with a base pressure of 5×10^{-9} Torr. The deposited films were 10 nm thick, and were transferred from the growth chamber into the UPS analysis chamber under UHV. The contact potential between the sample

and the detector limits the collection of low kinetic energy electrons. Hence, the thin film substrates were biased at either -3 V or -4 V to overcome this potential barrier.

The oxidation potentials of the sample molecules listed in Table 1, dissolved in dimethylformamide, acetonitrile, and dichloromethane (see Table 2 for their relative dielectric constants at room temperature [22]), were obtained versus a ferrocene/ferrocenium reference solute using differential pulse voltammetry, and using tetrabutylammonium hexafluorophosphate as the electrolyte. The solutions contained only micro-molar concentrations of the sample solutes to prevent shifts in oxidation potential due to concentration effects [5], and the voltage between the working and counter electrodes was swept at a scan rate of 100 mV/s. The working electrode was 0.2 cm in diameter by 1.5 cm long.

Only materials that could be reversibly oxidized (i.e. resulting in closed CV loops) were considered. In the context of electrochemistry, a reversible redox reaction is one where an electrogenerated intermediate is stable in the timeframe of the experiment. The reversible intermediate should have a half-life $> 10^{-2} \times (\text{scan rate})^{-1}$, where the scan rate is measured in V/s [23]. Neither aluminum tris(quinoline-8-olate) (Alq_3) nor aluminum(III) bis(2-methyl-8-quinolinato)4-phenylphenolate (BALq) undergo reversible oxidation. The potential given for these molecules is the irreversible anodic peak potential, the first peak of the CV trace. However, an irreversible peak potential may correspond to within 100 mV of the reversible oxidation potential if the species generated by a reversible electron-transfer process is consumed by a rapid, chemical follow-up reaction [24]. This may occur for both Alq_3 and BALq in the CV measurements.

5. Results and discussion

Both UPS and electrochemical methods have been used to determine the HOMO energies of materials incorporated into organic electronic devices. Only the UPS measurement provides a direct measure of the HOMO energy of a given compound in the solid-state. Electrochemical methods

Table 1
List of molecules studied and their associated oxidation and ionization energies

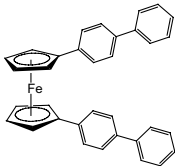
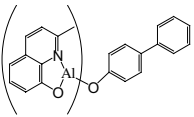
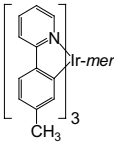
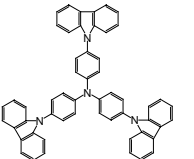
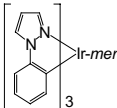
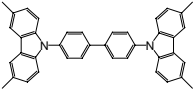
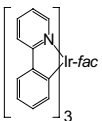
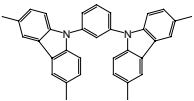
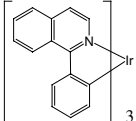
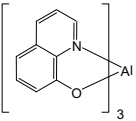
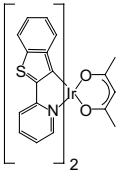
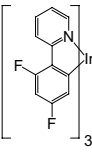
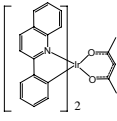
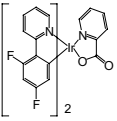
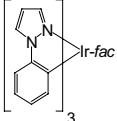
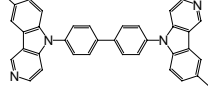
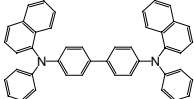
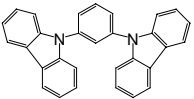
Electric potential/V (versus Fc/Fc ⁺ in DMF)	E_i /eV	Structural formula	Electric potential/V (versus Fc/Fc ⁺ in DMF)	E_i /eV	Structural formula
0.00	-4.76		0.68	-5.52	
0.18	-4.85		0.69	-5.71	
0.28	-5.11		0.72	-5.76	
0.31	-5.10		0.74	-5.61	
0.32	-5.07		0.75	-5.65	
0.36	-4.99		0.78	-5.68	
0.37	-5.07		0.89	-5.91	
0.38	-5.03		0.92	-5.99	
0.38	-5.30		1.00	-5.98	

Table 1 (continued)

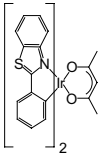
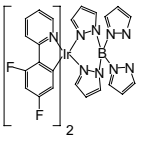
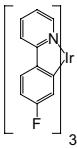
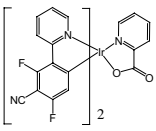
Electric potential/V (versus Fc/Fc ⁺ in DMF)	E_i /eV	Structural formula	Electric potential/V (versus Fc/Fc ⁺ in DMF)	E_i /eV	Structural formula
0.56	-5.33		1.08	-6.08	
0.56	-5.50		1.23	-6.36	

Table 2
Linear fits of E_{HOMO} versus V_{CV} for different solvents

	Dielectric constant at 300 K	s	V_{REF}
Dimethylformamide (DMF)	38.3	1.4 ± 0.2	3.2 ± 0.6
Acetonitrile (ACN)	37.5	1.4 ± 0.2	3.2 ± 0.7
Dichloromethane (CH ₂ Cl ₂)	9.1	1.2 ± 0.1	3.9 ± 0.5

require the use of a reference compound with measured oxidation potential (V_{CV}) and E_i values. Comparison of the oxidation potentials for the reference sample and unknown sample has been used to estimate the difference in E_i values for the two materials. The most common reference compound for such measurements is ferrocene, due to its highly reversible oxidation and the stability of both neutral and cationic forms in a wide range of solvents. The assumptions in this electrochemical method are that there is a one-to-one correspondence between shifts in oxidation potential and E_i and that the reference compound has well defined V_{CV} and E_i values, as shown previously for metal-free phthalocyanines [7]. We will show below that the one-to-one correspondence between shifts in V_{CV} and E_i is not valid. Additionally, the ferrocene reference solute commonly used in electrochemical studies does not have a well defined solid-state E_i value. The commonly used E_i value for ferrocene (4.8 eV) was inferred from theoretical electrochemical studies [25–27], which estimated the work function for a standard hydrogen electrode (SHE) as 4.6 V, and $V_{\text{CV}} = 0.2$ V versus SHE [28].

One reason for the difficulty in performing UPS measurements of a ferrocene thin film is the high volatility of the material, so cold substrate holders are required in a UHV environment [29]. The adiabatic ionization energy of ferrocene in the gas phase is reported to be 6.72 eV [30], and Ritsko et al. [29] have previously measured the thin film E_i of ferrocene to be 5.4 eV; however, that work provides no information on how the thin film is biased to avoid contact potential effects that occur in the experimental setup. The error caused by the contact potential is typically removed by applying a -3 V, relative to ground, bias to the sample, as is done in this study [3]. Without biasing the sample, the value of E_i is unreliable and could be larger than a value determined when the sample is biased. Thus, the experimental results obtained by Ritsko et al. on the solid-state samples of ferrocene are inconsistent with the results presented here, due to experimental considerations.

The volatility of ferrocene is substantially decreased by adding a biphenyl group to each of the cyclopentadienyl rings of the ferrocene molecule. The HOMO energy for this ferrocene derivative is 4.76 eV. The biphenyl substitution does not affect the oxidation potential of ferrocene, so the value determined here is a good estimate for the HOMO energy of ferrocene itself. Our measured E_i matches that previously estimated from electrochemical methods, supporting the use of this value for the ferrocene reference sample.

The E_{HOMO} of several representative electronic materials from families of organometallic

complexes [31–35], triarylaminines [36], and carbazoles [37] are plotted versus V_{CV} in Fig. 4. The molecular structural formulae, V_{CV} and E_{HOMO} of this family of molecules are listed in Table 1. There is a linear relationship between the two measurements, best fit by the single solid line, following

$$E_{HOMO} = -(1.4 \pm 0.1) \times (qV_{CV}) - (4.6 \pm 0.08) \text{ eV}, \quad (4)$$

with a linear regression correlation coefficient of 0.978.

In Fig. 3, s is plotted versus normalized distance of the solute molecules from the conductor, d/r , for two extreme conditions. For $\epsilon_{CV}/\epsilon_{film} = 1$, the discrepancy between the energy levels is solely due to image charge effects. In this case, it is assumed that monolayers of solute are formed on the surface of the electrode such that the immediate neighborhood of the solute molecules in CV differs from that of UPS only by the presence of the conducting electrode, thereby making the dielectric constants the same in both situations. Assuming close packing of spherical molecules next to the

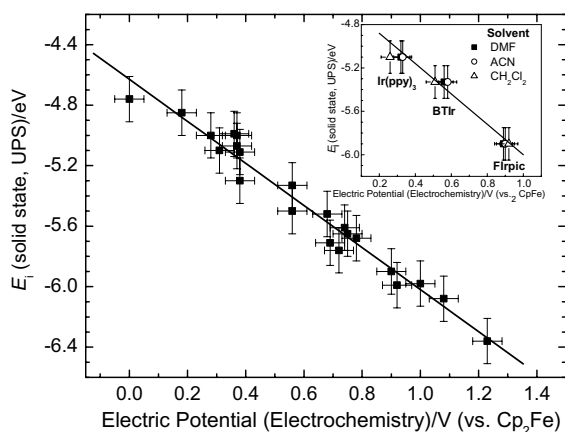


Fig. 4. HOMO energies (E_{HOMO}) determined using UPS versus relative oxidation potentials (V_{CV}) for several types of molecules: iridium and aluminum chelates, triarylaminines and carbazoles using dimethylformamide (DMF) as solvent and a ferrocene/ferrrocenium reference. The solid line is a best fit to the data following $E_{HOMO} = -(1.4 \pm 0.1)qV_{CV} - (4.6 \pm 0.08) \text{ eV}$. Inset: E_{HOMO} versus V_{CV} for the solvents DMF, acetonitrile (ACN) and dichloromethane (CH_2Cl_2) with a ferrocene/ferrrocenium reference sample. The solid line is the fit obtained with DMF as solvent.

working electrode, $d/r = 1.8 \pm 0.2$ (i.e. the value at $s = 1.4$) corresponds to 3.5 ± 0.7 monolayers. From the area under the second positive peak of the CV measurement (see shaded area in Fig. 2), we infer that $(4.5 \pm 0.5) \times 10^{14}$ molecules are oxidized per voltage scan with a voltage sweep rate of 100 mV/s. Given that the area of the working electrode is 0.94 cm^2 , and that each monolayer consists of $(1.4 \pm 0.4) \times 10^{14}$ molecules, we find that $r = 0.44 \pm 0.07 \text{ nm}$. Based on space-filling model calculations of Alq_3 , $\text{Ir}(\text{ppy})_3$, 4,4'-bis[*N*-(1-naphthyl)-*N*-phenyl-amino]biphenyl (NPD), and *N,N'*-dicarbazolyl-3,5-benzene (mCP), the volumes of these molecules are 0.540 nm^3 , 0.520 nm^3 , 0.645 nm^3 , and 0.438 nm^3 , respectively, corresponding to radii of 0.5 nm, 0.5 nm, 0.54 nm, and 0.47 nm, respectively, in agreement with the estimated value of $r = (0.44 \pm 0.07) \text{ nm}$.

For the case of $\epsilon_{CV}/\epsilon_{film} = 1.4$, the discrepancy between the energy levels is entirely due to the solvation effect. Hence, $f(r, d) \rightarrow 1$ as $d/r \rightarrow \infty$. In fact, for the cases studied here, $1 < \epsilon_{CV}/\epsilon_{film} < 1.4$, both solvation and image charges should be considered (Fig. 3, bold line).

Cyclic voltammetry data for three molecules were taken using two other solvents, acetonitrile (ACN) and dichloromethane with ferrocene/ferrrocenium as the reference sample in all cases. The V_{CV} for several molecules in these solvents are plotted against E_{HOMO} in the inset of Fig. 4, along with the fit obtained earlier with dimethylformamide (DMF) as the solvent. The fits for the individual solvents and their dielectric constants at room temperature are given in Table 2. The dielectric constants of dimethylformamide and acetonitrile are almost identical, and thus the oxidation potentials obtained are also similar. Although dichloromethane has a dielectric constant that is four times less than the other solvents, the change in s is only 15%, which is within experimental error. This suggests that the image charge effect has a more significant contribution to the slope than the solvation effect. Nevertheless, in all cases the fits are linear and are quantitatively consistent with the analysis in Section 2.

This model is based on molecules being spherical; a simplification that allows for an analytical expression of the image charge factor. In this case,

only d/r , along with the ratio of dielectric constants of the film to the solvent are required to accurately determine the HOMO energy from V_{CV} . Consideration of more complicated molecular shapes leading to higher order multipoles would involve other parameters such as molecular orientation with respect to the conductor. However, the accuracy afforded by such complications is insufficient to change the value inferred from the image charge factor. A detailed molecular orbital calculation to determine the energy levels of different redox states of the molecule would provide a better physical understanding of the dependence of the effective dielectric constant, ϵ_{CV} , on the dielectric constant of the solvent, ϵ_{Sol} , while taking into account the screening effects due to the supporting electrolyte. Nevertheless, the simplicity of the model presented here, along with the analysis of an extreme case of identical dielectric constants assumed in the UPS and CV experiments, is sufficient to conclude that the image charge factor, along with solvation effects, are all that are necessary to derive a quantitative relationship between the CV and UPS methods.

6. Conclusion

We have shown that a linear relationship exists between the HOMO energy found using UPS and the oxidation potential found from CV. This relationship is explained by a combination of solvation and image charge effects. The latter is quantified by approximating a molecule as a positive ion core surrounded by an electron cloud with an effective radius, r , inducing image charge in the conductive working electrode, and polarization of the electrolyte. We find that the two spectroscopic techniques are quantitatively related by $E_{HOMO} = -(1.4 \pm 0.1) qV_{CV} - (4.6 \pm 0.08) \text{ eV}$ for a wide range of organic electronic materials, where E_{HOMO} is directly measured from the UPS spectrum.

Acknowledgements

The authors are grateful to Prof. Antoine Kahn and Dr. Jason Brooks for helpful discussions. We

also thank Universal Display Corp. for partial support of this work.

References

- [1] S.T. Lee, Y.M. Wang, X.Y. Hou, C.W. Tang, *Appl. Phys. Lett.* 74 (1999) 670.
- [2] R.J. Holmes, B.W. D'Andrade, S.R. Forrest, X. Ren, J. Li, M.E. Thompson, *Appl. Phys. Lett.* 83 (2003) 3818.
- [3] A. Rajagopal, C.I. Wu, A. Kahn, *J. Appl. Phys.* 83 (1998) 2649.
- [4] J. Goodisman, *Electrochemistry: Theoretical Foundations, Quantum and Statistical Mechanics, Thermodynamics, The Solid State*, Wiley, New York, 1987.
- [5] D.T. Sawyer, A. Sobkowiak, J. Julian, L. Roberts, *Electrochemistry for Chemists*, first ed., John Wiley & Sons, New York, 1995.
- [6] E.V. Tsiper, Z.G. Soos, W. Gao, A. Kahn, *Chem. Phys. Lett.* 360 (2002) 47.
- [7] R.O. Loutfy, Y.C. Cheng, *J. Chem. Phys.* 73 (1980) 2902.
- [8] N. Sato, G. Saito, H. Inokuchi, *Chem. Phys.* 76 (1983) 79.
- [9] K. Seki, *Mol. Cryst. Liq. Cryst.* 171 (1989) 255.
- [10] H. Ishii, K. Sugiyama, E. Ito, K. Seki, *Adv. Mater.* 11 (1999) 605.
- [11] D. Cahen, A. Kahn, *Adv. Mater.* 15 (2003) 271.
- [12] A.J. Bard, L.R. Faulkner, *Electrochemical Methods. Fundamentals and Applications*, Wiley, New York, 1980.
- [13] J.O.M. Bockris, S.D. Argade, *J. Chem. Phys.* 49 (1968) 5133.
- [14] W.N. Hansen, D.M. Kolb, *J. Electroanal. Chem.* 100 (1979) 493.
- [15] A. Frumkin, B. Damaskin, *J. Electroanal. Chem.* 79 (1977) 259.
- [16] R. Gomer, G. Tryson, *J. Chem. Phys.* 66 (1977) 4413.
- [17] E. Chen, W.E. Wentworth, J.A. Ayala, *J. Chem. Phys.* 67 (1977) 2642.
- [18] D.E. Richardson, *Inorg. Chem.* 29 (1990) 3213.
- [19] M.F. Ryan, J.R. Eyster, D.E. Richardson, *J. Am. Chem. Soc.* 114 (1992) 8611.
- [20] Kurt J. Lesker, Pittsburgh, PA 15268.
- [21] S.R. Forrest, *Chem. Rev.* 97 (1997) 1793.
- [22] T.J. Bruno, P.D.N. Svoronos, *CRC Handbook of Basic Tables for Chemical Analysis*, CRC Press, Boca Raton, FL, 1989, p. 89.
- [23] L. Nadjo, J.-M. Savéant, *J. Electroanal. Chem.* 48 (1973) 113.
- [24] J.O. Howell, J.M. Goncalves, C. Amatore, L. Klasinc, R.M. Wightman, J.K. Kochi, *J. Am. Chem. Soc.* 106 (1984) 3968.
- [25] S. Trasatti, *Pure Appl. Chem.* 58 (1986) 955.
- [26] J. Pommerehne, H. Vestweber, W. Guss, R.F. Mahrt, H. Bassler, M. Porsch, J. Daub, *Adv. Mater.* 7 (1995) 551.
- [27] C.J. Bloom, C.M. Elliott, P.G. Schroeder, C.B. France, B.A. Parkinson, *J. Am. Chem. Soc.* 123 (2001) 9436.
- [28] H.M. Koepp, H. Wendt, H. Strehlow, *Z. Electrochem.* 64 (1960) 483.

- [29] J.J. Ritsko, P. Nielsen, J.S. Miller, *J. Chem. Phys.* 67 (1977) 687.
- [30] J.W. Rabalais, L.O. Werme, T. Bergmark, L. Karlsson, M. Hussain, K. Siegbahn, *J. Chem. Phys.* 57 (1972) 1185.
- [31] J.F. Ambrose, L.L. Carpenter, R.F. Nelson, *J. Electrochem. Soc.* 122 (1975) 876.
- [32] C.H. Chen, J.M. Shi, *Coord. Chem. Rev.* 171 (1998) 161.
- [33] S. Lamansky, P. Djurovich, D. Murphy, F. Abdel-Razzaq, R. Kwong, I. Tsyba, M. Bortz, B. Mui, R. Bau, M.E. Thompson, *Inorg. Chem.* 40 (2001) 1704.
- [34] S. Lamansky, P.I. Djurovich, F. Abdel-Razzaq, S. Garon, D.L. Murphy, M.E. Thompson, *J. Appl. Phys.* 92 (2002) 1570.
- [35] A.B. Tamayo, B.D. Alleyne, P.I. Djurovich, S. Lamansky, I. Tsyba, N.N. Ho, R. Bau, M.E. Thompson, *J. Am. Chem. Soc.* 125 (2003) 7377.
- [36] B.E. Koene, D.E. Loy, M.E. Thompson, *Chem. Mater.* 10 (1998) 2235.
- [37] K.R.J. Thomas, J.T. Lin, Y.T. Tao, C.W. Ko, *J. Am. Chem. Soc.* 123 (2001) 9404.